APPENDIX 1
DUPONT BASIC PLUME MODEL

TABLE OF CONTENTS

DuPont Basic Plume Model

CONTENTS
(CONTINUED)

LIST OF FIGURES

1.0   GENERAL DESCRIPTION

The DuPont Basic Plume Model calculates the time-dependent lateral movement of waste plumes emanating from various wells at an injection site. Key features of the model were discussed by Miller et al. (1986).

2.0   MODEL STRUCTURE

The model is set up as a single layer calculation and neglects vertical exchange of fluids between geological strata. A separate calculation is therefore required for each layer into which waste is injected.

Many particle-tracking models of this type neglect the effects of non-uniformities within the injection formation on the distribution of the waste. Such non-uniformities are found to give rise to the phenomenon of macro-dispersion, which causes the leading edge of the waste plume to be jagged or diffuse (rather than vertical and sharp) and results in a greater effective lateral extent for the plume. The Basic Plume Model accounts for the effects of non-uniformities by means of a special technique, known as the "multiplying factor concept," introduced by Miller et al. (1986). This concept provides the basis for establishing an extreme outer perimeter beyond which none of the waste could have passed.

3.0   MODEL INPUTS

The model inputs are the set of parameters that must be supplied to the computer program to perform a site-specific calculation of waste transport within the injection stratum. In addition to identifying the required parameters, the present discussion considers the potential sources of this data and the sensitivity of the model results to variations in the inputs.

3.1   Well Locations

The geographical coordinates of all wells are specified using an X-Y coordinate system inscribed onto a map of the site locale. Data on the locations of the wells is readily available from historical records and maps of the plant vicinity. For a non-vertical wellbore, the borehole is projected downward to its intersection with the injection horizon.

The uncertainties associated with specifying the well locations are typically quite minimal and will have virtually no influence on the predicted advance of the waste plumes.

3.2   Geological Data

3.2.1   Average Injection Stratum Thickness

Average thickness of the injection stratum is determined by analyzing resistivity and spontaneous potential logs. Special geological surveys by experienced consultation organizations are often used as additional data sources.

The model predicts that the distance the waste front advances laterally is inversely proportional to the square root of the injection stratum thickness for the case of an isolated well in an unbounded isotropic medium.

3.2.2   Average Injection Stratum Porosity

The average porosity of the injection stratum is determined from core samples or regional geological studies of the area near the injection site. A large number of core samples is desirable to obtain a representative average.

The lateral advance of the waste front predicted by the model is inversely proportional to the square root of the porosity for the case of an isolated well in an unbounded isotropic medium. This is identical to the variation noted above with respect to the injection stratum thickness.

3.2.3   Location of Flow Barriers

The effects of barriers to fluid flow are accounted for explicitly in the model using the method of image wells (Freeze and Cherry, 1979). The model represents these features as vertical planar boundaries of infinite extent. Their location and orientation are supplied to the model by providing the lateral coordinates of any two points along the flow barrier. The model then calculates the appropriate locations of all image wells by applying a simple geometric formula. Information on the presence of flow barriers can be obtained from geological surveys of the site.

3.2.4   Multiplying Factor

The multiplying factor is used in the Basic Plume Model to compensate for the effects of dispersion associated with non-uniformities in the injection stratum and other geological uncertainties that may be present. It provides a basis for establishing a conservative outer boundary to the possible lateral extent of the waste, rather than predicting the exact waste location.

In practice, the multiplying factor functions as a scaling parameter that increases (mathematically) the injection rates input to the model at the various wells by a constant factor equal to or greater than 1. This results in a corresponding increase in the predicted lateral extent of the waste plumes, relative to the case of a perfectly homogeneous formation. The increased lateral movement simulates, on firm theoretical grounds, the enhanced transport that results from non-homogeneities. Thus, the multiplying factor concept enables a transport model that has been structured primarily as a tool for homogeneous porous media to be used to predict waste movement in a non-homogeneous geological system.

To account for the effects of vertically stratified permeability variations through the thickness of the injection formation, the multiplying factor is set equal to the ratio of the maximum horizontal permeability to the horizontal permeability averaged over the formation thickness. Values for these parameters can be obtained from core samples taken from the injection stratum during well drilling or from samples at neighboring wells. A large number of samples is desirable to obtain statistically significant estimates.

Use of the multiplying factor guarantees a margin of safety in the calculations, since the approach neglects the mitigating influence of both small-scale transverse dispersion and slow vertical flow, each of which acts to retard the lateral transport.

In calibrating the Basic Plume Model to actual field data, the multiplying factor is employed as the primary calibration parameter. Its value is adjusted to match the observed history of waste movement in the subsurface, as determined from encounters or nonencounters of waste at newly drilled wells at a site.

The predicted lateral advance of the waste front in the Basic Plume Model is proportional to the square root of the multiplying factor for the case of an isolated well in an unbounded medium.

3.3 Site Injection History

The waste injection history at each well must be specified as a function of time. If wells are operated such that only one horizon is perforated at any time, the flow into the injection stratum will be identical to the injection rate at the wellhead. For a well perforated into more than one horizon at a time, the total injection flow rate at the wellhead is known in advance, but not the partitioning of the flow between the perforated horizons. This partitioning can be calculated using the Multi-layer Pressure Model described in Appendix VII-2.

The well injection histories and the sequence of well completions are specified as functions of time for input to the Multi-layer Pressure Model. Injection history information is available from the site operating records. It can be provided on an average annual basis, or preferably, on an average monthly basis.

4.0   MODEL OUTPUTS

The model calculates the time-dependent motion of the front between the waste and formation fluid by predicting the movement of a set of fictitious tracer particles situated at the leading interface of each plume. The plume shapes can then be displayed graphically by joining the points along the plume boundaries.

5.0   ASSUMPTIONS, VALIDATIONS, AND MARGINS OF SAFETY

This section describes the key assumptions in the model and evaluates the particular site-specific conditions under which the assumptions are valid.

5.1   The Flow Is Incompressible

The effects of compressibility of the fluids and the porous medium are important in determining the pressure distribution in a broad geographic area surrounding an injection site, but not in determining the location of the waste. This is because the actual compression of materials that takes place locally is very small but is distributed over a large lateral area. The compression effect will amount to only a few tenths of a percent within the region occupied by the waste. Therefore, neglecting this compression must result in only a slight inaccuracy in the prediction of the waste location. Since the waste is compressed and the pores of the rock are expanded, the assumption will always lead to an underestimate in the lateral extent of the waste plume.

5.2   Seepage from the Injection Stratum into the Overlying and Underlying Aquitards Is Negligible

The adjacent aquitards are typically very low in permeability and will thus permit only a small amount of seepage to occur from the injection stratum. Moreover, this loss will result in a reduction in the lateral flow velocity and in the horizontal extent of the waste plume. Therefore, this assumption is conservative from the standpoint of bounding the waste movement.

5.3   Properties of the Injection Stratum do not Vary with Position

The model assumes that the thickness of the injection stratum does not vary horizontally, and that the permeability and porosity are constant with both horizontal and vertical position.

Horizontal variations in formation thickness and permeability can affect the lateral extent of waste transport. Large, sudden changes in these parameters can be included explicitly in the model calculations, using image well techniques, or through the use of the multiplying factor.

In geological formations such as those in the Gulf Coast region, permeability can vary greatly with vertical location through the thickness of the stratigraphic units. This permeability variation can result in an inter-fingering phenomenon at the leading edge of the waste plume and the enhancement of lateral transport, sometimes referred to as macro-dispersion. Using the

DuPont Basic Plume Model

multiplying factor concept allows compensation for these effects and leads to an upper-bound estimate to the lateral movement of the waste.

5.4   Densities of the Waste and Formation Fluids Are Equal

Whenever the density of the injected waste differs from that of the native brine, there will be a tendency for natural convection effects to play a role in influencing the fluid flow velocities within the injection stratum. The injected fluid will be prone to either rise to the top of the formation or sink to the bottom, depending on whether it is more or less dense than the formation fluid. In addition, its leading edge will tend to move further horizontally than if the two fluids were of equal density, irrespective of which fluid is more dense.

Miller et al. (1986) assessed the magnitude of these effects. They showed that by applying an appropriately selected multiplying factor, the influence of density variations between the waste and formation fluids can be included within the context of the Basic Plume Model.

For those injection sites where the multiplying factor has been calibrated to the observed history of waste encounters and nonencounters at newly drilled wells, the value obtained will inherently include the effects of density differences between the waste and formation fluids.

5.5   The Fluid Viscosity Is Uniform within the Injection Stratum

Fluid viscosity within the injection stratum will typically vary by less than a factor of two between the waste viscosity in the region near the wells to the formation fluid viscosity at distances beyond the waste plumes. For a single-well injection site, these variations will have virtually no influence on the radial transport of waste (although the pressure distribution will be affected). For a multiple-well site, the effects can normally be neglected. However, if viscosity variations are much larger than a factor of two at a multiple-well site, appropriate compensation should be included in transport calculations. This can be accomplished by judicious choice of the multiplying factor in the Basic Plume Model.

5.6   The Injection Stratum Is Fully Perforated

Most injection wells are not perforated over the full height of the injection interval. The effects of partial perforation will typically be manifested as a localized phenomenon, confined to the horizontal region within a few formation heights of each individual well. The presence of partial perforation at one well will normally not significantly influence the transport at adjacent wells.

The distance waste travels laterally can be expected to be slightly enhanced as a result of partial perforation, but the effect can be neglected. For a homogeneous isotropic injection stratum, one can show that the lateral advance of the waste plume will never exceed that obtained with a fully perforated interval by more than one-fourth the formation height. This maximum enhancement will occur at a lateral distance of about half a formation height away from the injection well. At larger distances from the well, the waste front will tend to become "self-sharpening," and revert to a more nearly vertical configuration. Thus, the enhancement resulting from partial perforation will decrease with increasing distance from the well.

If the injection formation is anisotropic, so that the permeability in the vertical direction is considerably smaller than the permeability in the horizontal [for example, in a formation exhibiting "layered anisotropy" (Freeze and Cherry, 1979)], the enhanced lateral transport produced by partial perforation will be greater than that described above in the case of an isotropic system. For this situation, one can show that the increased lateral transport will never exceed one-fourth the formation height multiplied by the square root of the ratio of the horizontal to the vertical permeability. Even for a permeability ratio of 10, this will amount to an increased lateral advance of only about three-fourths of a formation height.

6.0   FORMULATION AND SOLUTION

This section presents the formulation and solution of the Basic Plume Model. Attention is focused first on the case of a purely homogeneous geological formation, which produces an ideal vertical waste front. Second, the effects of non-uniformities and hydrodynamic dispersion are considered. Finally, some novel numerical techniques are presented which overcome certain computational problems frequently arising in calculations of this type.

6.1   Ideal Sharp Vertical Waste Front

In a purely homogeneous geological formation, the interface between the waste and formation fluid will advance laterally as a sharp vertical front. This front will take the shape of a right circular cylinder for the case of a single isolated well. The diameter of the circle will be determined strictly by geometric considerations, involving the total volume of the injected waste, and the height and porosity of the formation. Such a plume is referred to as an ideal circular waste plume.

For multiple-well injection sites, methods of analyzing waste transport in purely homogeneous geological formations have been available for many decades, based on work in the petroleum field (Collins, 1961). The Basic Plume Model is therefore not a new development, but closely parallels the standard approach recommended by others (Collins, 1961; Javandel et al., 1984).

The standard approach involves a two-part process. First, determine lateral velocity distribution within the injection formation at any time using solutions provided by potential flow theory. Second, integrate the time-dependent kinematic equations relating the calculated velocity distribution to the motion of the interfacial front between the waste and formation fluid.

The first step takes advantage of the well-known mathematical analogy between fluid flow in porous media and ideal potential flow of inviscid fluids. This mathematical analogy permits the determination of the velocity distribution in an injection formation directly from the previously established solution to the same problem in potential flow theory.

For waste injection at a multiple-well site, Javandel et al. (1984) gave the following potential flow expressions for the lateral components of fluid velocity in an injection formation.

$$V_x = \frac{1}{2\pi\phi b} \sum_{i=1}^{N} \frac{Q_i\,(x - x_i)}{(x - x_i)^2 + (y - y_i)^2} \tag{1}$$

$$V_y = \frac{1}{2\pi\phi b} \sum_{i=1}^{N} \frac{Q_i\,(y - y_i)}{(x - x_i)^2 + (y - y_i)^2} \tag{2}$$

Where:

v_x and v_y	=	Lateral pore velocities in the x and y horizontal coordinate directions
Q_i	=	Instantaneous injection rate at time t at well i
x_i and y_i	=	Coordinates of well i
b	=	Height of the injection formation
ϕ	=	Porosity
N	=	Total number of injection wells

Equations 1 and 2 implicitly include the use of linear spatial superposition principles to generate the velocity distribution for multiple injection wells from the simpler pure radial velocity distribution for a single isolated well.

The second part of the modeling process involves the use of the velocities determined by Equations 1 and 2 to calculate the time-dependent motion of the front between the waste and formation fluid. This is accomplished mathematically by introducing a set of fictitious tracer particles around the circumference of each plume, and calculating the trajectory of these particles as time progresses (see Figure 1). A separate set of tracer particles is employed for each plume. Because the model automatically conserves mass, these tracer particles remain situated on the outer perimeter of the plume for all times.

The kinematic equations for calculating the time-dependent motions of the tracer particles are given by

$$\frac{dX_k}{dt} = v_x\left(x_k, y_k\right) \tag{3}$$

$$\frac{dY_k}{dt} = v_y\left(x_k, y_k\right) \tag{4}$$

Where:

X_k and Y_k	=	The horizontal spatial coordinates of a fictitious tracer particle k (k = 1....M, where M is the total number of particles around the circumference of the plume) at time t.

Substitution of Equations 1 and 2 into Equations 3 and 4 leads to a pair of coupled first order ordinary differential equations for the horizontal spatial coordinates X_k and Y_k of each tracer particle as parametric functions of time. The model integrates these equations numerically for all of the particles along the boundaries of all the plumes using a commercially available non-stiff ordinary differential equation routine. This determines the location of the particles around the circumference of each plume at any time t. The shape of the plume can then be displayed graphically by connecting the points.

6.2 Effects of Non-uniformities and Hydrodynamic Dispersion

The degree of hydrodynamic dispersion occurring in field-scale transport experiments has frequently been observed to be much greater than that measured in homogeneous porous media under laboratory conditions.[1] The cause of this phenomenon has been associated with the existence of significant heterogeneous variations in material properties within the underground geological formations, particularly of permeability.

Another important phenomenon that has been noted in the field is the dependence of the effective longitudinal dispersivity parameter (dispersivity in the direction of fluid movement) on the scale of measurement.[2] The observed dispersivity has been found to increase monotonically with distance between the injection source and the measurement receptor. This observation is inconsistent with the usual theoretical assumption employed in many transport models (Intercomp, 1976), namely, that the dispersivity is a constant.

A number of recent publications have provided greater insight into these dispersion phenomena and have reconciled many of the apparent inconsistencies.[3] By focusing attention on purely stratified geological formations in which the permeability varies strongly with vertical position but not with location laterally, these studies were able to show that at relatively small distances from the injection source, the transport behavior is dominated by advection rather than dispersion. The advection referred to here includes the effects of the vertical permeability variations which give rise to corresponding variations in the lateral velocity profile (Figure 2). These velocity variations cause a highly interfingered boundary to develop between the injected fluid and the native liquid.

---

[1]   Guven et al., 1984; Fried and Combarnous, 1971; Pickens and Grisak, 1981a and 1981b.
[2]   Guven et al., 1984 and 1985; Anderson, 1979 and 1984; Molz et al., 1983; Domenico and Robbins, 1984; and Gillham et al., 1985; Mercado, 1984.
[3]   Guven et al., 1984 and 1985; Molz et al., 1983; Matheron and De Marsily, 1980; Lake and Hirasaki, 1981.

When samples are then taken at a collection receptor, the time-dependent concentration variations observed are incorrectly interpreted as being caused by dispersion. In reality, they are caused by the effects of the *advective interfingering*, combined with the vertical mixing that takes place during the sampling process. The effective field-scale *pseudo-dispersivity* (sometimes called *macro-dispersivity*) deduced from this type of test is typically much larger than the dispersivity measured for homogeneous core samples in the laboratory. In the region dominated by advective interfingering, the pseudo-dispersivity determined in the field will be scale-dependent and will increase with increasing distance between the tracer source and the collection receptor.

At larger lateral distances between the source and receptor, a second transport mechanism begins to take effect (Figure 3). This mechanism is *small-scale transverse dispersion*, perpendicular to the advective concentration fingers (in the vertical direction normal to the motion). Note that until the concentration fingers have formed, this second mechanism cannot occur since the driving force for transverse dispersion is a concentration gradient in the vertical direction. The transverse dispersion mechanism acts in opposition to the advective interfingering effect by allowing solutes to transfer from the faster moving layers to the slower moving layers (fingers) and vice versa. The net effect is to reduce the rate at which the pseudo-dispersivity increases with the increasing scale of measurement, and thus the value of the pseudo-dispersivity attained at any location.

At very large lateral distances between an injection source and a measurement receptor, the interaction between the two opposing transport mechanisms approaches an equilibrium. This causes the longitudinal macro-dispersivity to no longer increase with increasing scale of measurement, and to attain a final constant field scale value. On this scale, the concentration variations at the front between the injected fluid and the native liquid will resemble the variations caused by ordinary dispersion, rather than advection. The concentration fingers will have largely vanished.

The combination of an advective velocity variation normal to the direction of motion and small-scale transverse dispersion typically manifests itself as an apparent longitudinal dispersion phenomenon. This is analogous to the effective longitudinal dispersion behavior investigated by G. I. Taylor (1953, 1954) for flow in a tube. The effect is often referred to as "Taylor dispersion."

The implications of these findings on the lateral transport of waste in underground injection systems can be very significant. Large non-uniformities in properties within the injection stratum (mainly non-uniform permeability) can lead to a high degree of macro-dispersion at the front

between the waste and the native brine. Such non-uniformities can be broken down into two broad categories - horizontal and vertical.

A variety of different forms of horizontal variation can occur, but two of the most common are:

1. Gradual changes in permeability, and
2. Sudden changes, such as a flow barrier.

If a sudden change is known to exist, its effects can be modeled directly using image well methods as previously discussed. Gradual trends have less of an influence on waste transport but are more difficult to model precisely. However, one can obtain a worst-case estimate of their effects simply by approximating these variations as equivalent sudden changes. Other types of horizontal variations that may be present can be handled through the use of the multiplying factor to provide a margin of safety in predicting an upper bound to the maximum lateral extent of the waste.

In the Gulf Coast region, the permeability may vary strongly with vertical position through the thickness of the geological formations (Figure 4). Moreover, these vertical variations appear to persist over large lateral distances. In such a system, the interface between the waste and the native brine will no longer be perfectly flat and vertical as in the ideal case of a homogeneous porous medium. Instead, it will assume a highly interfingered shape in which the advective transport mechanisms discussed previously are at work. Neglecting the mitigating influence of the small-scale transverse dispersion mechanism in limiting the horizontal extent of waste provides a conservative worst-case estimate of the lateral waste transport.

The quantitative implications of this permeability distribution are illustrated schematically in Figure 5 for the simple case of rectilinear flow. In the system shown, horizontal flow takes place within a slab of porous matrix of finite extent consisting of a series of discrete layers, each with a different permeability. The flow is driven by an applied pressure difference between the two ends of the slab. This system is analogous to an electric circuit consisting of a set of unequal resistors connected in parallel across a constant potential. The fluid flow will distribute itself among the different layers such that highest flow rates will be obtained in the layers of least resistance (highest permeability). This results in a velocity distribution across the slab that directly reflects the permeability variation:

$$\frac{v(z)}{\bar{v}} = \frac{k(z)}{\bar{k}} \qquad (5)$$

Where $\bar{v}$ and $\bar{k}$ are the horizontal velocity and permeability averaged over the thickness of the slab, and v(z) and k(z) are the local values at vertical position z.

According to Equation 5, velocity variations are determined not by the magnitude of the permeability, but by the variations in permeability relative to the average. This represents an important difference between a model used for calculating transport in a stratified geological system (such as the present Basic Plume Model) and a model used for calculating the pressure distribution (such as the Multi-layer Pressure Model), in which the response is determined primarily by the vertically-averaged permeability.

The results expressed in Equation 5 are valid, not just for the simple case of rectilinear flow, but for all geological arrangements in which permeability varies solely with vertical position through the formation. Therefore, these results can be applied directly to predict waste transport within any vertically-stratified multiple-well injection system. For example, to calculate the location of the interface between the waste and native brine in the fastest moving layer of waste, the average velocities determined in the Basic Plume Model are simply multiplied by the ratio of the maximum layer permeability to the vertically-averaged permeability. This is done most conveniently by scaling the injection rates input to all the wells in the model by this same ratio. Since the equations for the velocities are linear in the injection rates (see Equations 1 and 2), the procedure will automatically deliver the required velocity distribution for the fastest moving layer. When the model is run with this modification to the input data, it will output the time-dependent advance of the fastest moving layer of waste. Of course, only a small fraction of the total waste will actually travel this far.

6.3   Improved Numerical Procedures

A numerical difficulty sometimes experienced with "particle tracking" models like the Basic Plume Model is related to the tangential motion of the fictitious tracer particles along the boundary between the waste and formation brine. Although the particles are initially placed uniformly around the plume perimeter, they will tend to slide along the interface and accumulate in a limited portion of the front as the solution evolves. This leaves the coverage in some parts of the perimeter very sparse and causes a loss of resolution in displaying the plume boundary graphically. There is no loss of accuracy in the solution, only in the graphical display. This difficulty arises when two injection wells are situated relatively close to one another, so that the tracer particles in the "stagnation zone" between the wells are driven out of the region and forced toward the opposite sides of the plumes.

A novel approach has been developed in the Basic Plume Model to overcome these difficulties. This approach automatically requires that the tracer particles remain uniformly spaced around the perimeter of the plume for all times.

The new technique recognizes that the velocity of any tracer particle on the plume boundary can be resolved into two components, one perpendicular to the boundary and one tangential. Only the component perpendicular to the boundary is actually responsible for the observed advance of the plume. The tangential component merely causes the particles to slide along the perimeter like rings on a shower rod. Therefore, the tangential velocity components of the particles can be modified in any arbitrary manner without affecting the predicted shape and movement of the plume boundary. This forms the basis for the new computational approach to achieving high display resolution on the perimeter shape.

The objective of this derivation is to identify a modified velocity distribution (along the boundary of the plumes) capable of correctly predicting the time-dependent evolution of the boundary shapes, while continually maintaining the tracer particles at a uniform spacing around the perimeter. This is accomplished by defining a modified velocity variation $\underline{V}$ (underbars are used here to denote vectors) in the following form:

$$\underline{V} = \underline{v} + v * \underline{\tau} \qquad (6)$$

Where:

$\underline{v}$ =   Actual velocity of fluid movement determined from Equations 1 and 2

$\underline{\tau}$ =   Unit tangent vector to the plume boundary at each location

$v*$ =   Magnitude of an as yet undetermined alteration mathematically imposed on the tangential velocity

From the previous discussion it follows that if all the fictitious tracer particles move with this modified velocity variation, they will automatically remain situated on the plume boundary for all times and properly trace out the time-dependent motion of the perimeter. The problem then reduces to one of determining the variation in altered tangential velocity parameter $v*$ such that the spacing between the particles always remains uniform.

Assume that at time zero, when a well first begins injecting waste, particles are placed uniformly around the circumference of the injection well. Let θ denote the initial angular location of each particle with respect to the x coordinate direction. In the present development the parameter θ shall be used as a particle label or material coordinate to help keep track of the trajectories of the

individual particles as they pass through space. The spatial coordinates of any particle X and Y can be expressed parametrically as a function of the initial angle θ and time t as follows:

$$X = X\left(\theta, t\right)$$

$$Y = Y\left(\theta, t\right)$$

Next, denote dl as the differential arc length between two neighboring tracer particles along the plume boundary at time t. The material coordinates of the two tracer particles are q and q + dθ, and the length of the differential arc is given by:

$$dl = \sqrt{\left(X'\right)^2 + \left(Y'\right)^2}\; d\theta \tag{7}$$

Where:

$$X' = \frac{\partial X\left(\theta, t\right)}{\partial \theta} \tag{8}$$

And:

$$Y' = \frac{\partial Y\left(\theta, t\right)}{\partial \theta} \tag{9}$$

The rate at which this arc is growing in length (stretching) with respect to time is obtained by taking the time derivative of Equation 7. This yields:

$$\frac{dl}{dt} = \frac{X'V'_x + Y'V'_y}{\sqrt{\left(\left(X'\right)^2 + \left(Y'\right)^2\right)}}\, d\theta \tag{10}$$

Where V_x and V_y are the components of the modified velocity vector $\underline{V}$ defined in Equation 6, and where use has been made here of the fundamental kinematic conditions that:

$$V_x = \frac{\partial X\left(\theta,\ t\right)}{\partial t}$$

And:

$$V_y = \frac{\partial Y(\theta,\, t)}{\partial t}$$

The rate of stretching of the entire circumference of the plume, denoted C, is obtained by adding together the contributions of the individual differential elements of arc to yield:

$$\frac{dC}{dt} = \int_0^{2\pi} \frac{X'V'_x + Y'V'_y}{\sqrt{(X')^2 + (Y')^2}}\, d\theta \tag{11}$$

In order for the tracer particles to remain uniformly distributed around the circumference, the local rate of stretching of the differential arc length at any arbitrary location along the plume perimeter (per unit initial angle dθ) must match the average stretch rate existing over the entire circumference.

This requires that:

$$\frac{X'V'_x + Y'V'_y}{\sqrt{(X')^2 + (Y')^2}} = \frac{1}{2\pi} \int_0^{2\pi} \frac{X'V'_x + Y'V'_y}{\sqrt{(X')^2 + (Y')^2}}\, d\theta \tag{12}$$

If Equation 6 for the modified velocity variation $\underline{V}$ is next expressed in component form, one obtains:

$$V_x = v_x \frac{v^* X'}{\sqrt{(X')^2 + (Y')^2}} \tag{13}$$

$$V_y = v_y \frac{v^* Y'}{\sqrt{(X')^2 + (Y')^2}} \tag{14}$$

Where use has been made here of the fact that the components of the unit tangent vector $\underline{\tau}$ are given by:

$$\tau_x = \frac{X'}{\sqrt{(X')^2 + (Y')^2}}$$

$$\tau_y = \frac{Y'}{\sqrt{(X')^2 + (Y')^2}}$$

Substituting Equations 13 and 14 into Equation 12, and performing some straightforward mathematical manipulations yields:

$$\frac{dv^*}{d\theta} = \frac{1}{2\pi} \int_0^{2\pi} \frac{X'v'_x + Y'v'_y}{\sqrt{(X')^2 + (Y')^2}} d\theta - \frac{X'v'_x + Y'v'_y}{\sqrt{(X')^2 + (Y')^2}} \tag{15}$$

Equation 15 provides the desired relationship for determining alterations to the tangential velocity along the plume v* required for the tracer particles to remain uniformly spaced at all times. It expresses this velocity alteration in terms of the actual fluid velocity components v_x and v_y, and the local spatial derivatives of the plume shape. This velocity variation is not unique, since Equation 15 gives only the derivative of v*, rather than v* itself. As a result, the tangential velocity change is determined only up to an arbitrary constant of integration (v* at $\theta = 0$).

The required condition of equal spacing for the tracer particles will always be satisfied using Equation 15, irrespective of the choice for the integration constant. However, the average speed at which the equally spaced tracer particles move around the plume boundary will depend on the value selected. To establish uniqueness, it is reasonable to require that this average tangential speed be set equal to zero. This will prevent the particles from moving around the circumference of the plume like cars on a race track.

The average tangential speed will equal zero whenever the following condition is satisfied:

$$\int_0^{2\pi} \left(V_x X' + V_y Y' \right) d\theta = 0 \tag{16}$$

If Equations 13 and 14 for the components of the modified velocity vector $\underline{V}$ are substituted into Equation 16, one obtains:

$$\int_0^{2\pi} v^* \sqrt{(X')^2 + (Y')^2} \, d\theta = 0 \tag{17}$$

Where use has been made here of the condition that for potential flow, the integral in Equation 16 is identically zero (the flow is irrotational).

Equations 15 and 17 provide the required relationships in the Basic Plume Model for uniquely determining the tangential velocity parameter v*. Equation 17 is equivalent to specification of the constant of integration in Equation 15, or equivalently, the initial v* value at $\theta = 0$.

Both Equation 15 and Equation 17 can be simplified somewhat by recognizing that, since the tracer particles remain equally spaced around the plume boundaries at all times, the quantity

$$\sqrt{(X')^2 + (Y')^2}$$

will be a constant, independent of location on the perimeter (independent of θ). Therefore, this radical can be factored out of the integrals in Equations 15 and 17, to yield:

$$C\frac{dv*}{d\theta} = \int_0^{2\pi} \left(X'v'_x + Y'v'_y\right)d\theta - 2\pi\left(X'v'_x + Y'v'_y\right) \tag{18}$$

$$\int_0^{2\pi} v*d\theta = 0 \tag{19}$$

Where C is the circumference of the plume, defined as:

$$C = \int_0^{2\pi} \sqrt{(X')^2 + (Y')^2}\, d\theta \tag{20}$$

Similarly, Equations 13 and 14 become:

$$V_x = v_x + \frac{2\pi v* X'}{C} \tag{21}$$

$$V_y = v_y + \frac{2\pi v* Y'}{C} \tag{22}$$

Equations 18 through 22 are the relationships employed in the Basic Plume Model to obtain a uniform distribution of tracer particles and correspondingly high plotting resolution on the plume shapes.

DuPont Basic Plume Model

7.0   VERIFICATION

The computer program used to solve model equations has been verified against a variety of analytic and numerical solutions in the literature and by independent numerical tests to guarantee that it delivers correct and accurate results.

The single-well capabilities of the model were first compared with the analytic solution to the case of a homogeneous isotropic injection stratum. This analytical solution is given by the well-known equation:

$$r = \sqrt{\frac{V}{\pi \phi b}} \tag{23}$$

Where r is the radial distance from the well to the leading edge of the waste plume at any time, and V is the total volume of waste injected. The numerical model accurately duplicated this result to within 0.01 percent in all cases tested, irrespective of the injection rate history imposed.

To evaluate the ability of the computer program to accurately describe the behavior of multiple-well injection sites, calculations were performed on a system featuring two wells - an injection well and a nearby withdrawal well. The objective of the calculation was to predict the time-dependent movement of a waste front away from the injection well, and the time for the waste plume to exhibit "break-through" at the withdrawal well. This system was solved analytically by Muskat (1946), and numerically by Collins (1961) and Javandel et al. (1984). Collins considered the general case, in which the variables are expressed in dimensionless form, while Javandel et al. performed calculations for a specific field example. Muskat derived the following analytical expression for calculating the time at break-through:

$$t = \frac{\pi \phi d^2 b}{3Q} \tag{24}$$

Where d is the distance between the wells and Q is the injection rate.

The specific field arrangement analyzed by Javandel et al. (1984) is shown in Figure 6. They assumed an injection rate of 50 m^3/h at Well A, and an equal withdrawal rate at Well B. The height of the formation was 10 m, and the porosity was 25 percent ($\theta = 0.25$). Figure 7 shows a comparison between the results obtained by Javandel et al. (1984) and those from the Basic Plume Model. The agreement is excellent. The calculated break-through time using the Basic Plume

DuPont Basic Plume Model

Model was 4.30 years, which is identical to the value obtained by Javandel et al. (1984) and virtually indistinguishable from the analytic result.

The novel numerical technique developed for obtaining high plotting resolution on the shape of the waste plumes was tested by comparing results obtained with this procedure for complex multiple-well injection sites against corresponding calculations carried out using the standard approach. In all cases, the plots were superimposable. The new approach, however, provided much higher resolution in the critical regions near stagnation points.

Another test of the new high resolution version of the Basic Plume Model was to compare the calculated shapes of waste plumes for wells located adjacent to one another. The new numerical technique calculates each waste plume separately and uses the spatial derivatives of the individual boundary shapes over all positions on the plume perimeters to determine the motions of the tracer particles. In those specific cases where virtually all the formation fluid is squeezed out from between the plumes, the shapes of the plume boundaries should closely match one another. This condition has been found to prevail in all situations tested, to such an extent that the plumes fit together like pieces of a jigsaw puzzle.

REFERENCES

Anderson, M. P., 1979. Using Models to Simulate the Movements of Contaminants Through Groundwater Flow Systems, Crit. Rev. Environ. Contr., Vol. 9, pp. 97-156.

Anderson, M. P., 1984. Movement of Contaminants in Groundwater: Groundwater Transport Advection and Dispersion, in Groundwater Contamination, pp. 37-45, National Academy Press, Washington, DC.

Collins, R. E., 1961. Flow of Fluids Through Porous Media, Reinhold, New York.

Domenico, P. A., and G. A. Robbins, 1984. A Dispersion Scale Effect in Model Calibrations and Field Tracer Experiments, J. Hydrol., Vol. 70, pp. 123-132.

Freeze, R. A., and J. A. Cherry, 1979. Groundwater, Prentice-Hall, Englewood Cliffs, New Jersey.

Fried, J. J., and M. A. Combarnous, 1971. Dispersion in Porous Media, edited by V. T. Chow, in Advances in Hydroscience, Vol. 9, pp. 169-282, Acamemic, New York.

Gillham, R. W., E. A. Sudicky, J. A. Cherry, and E. O. Frind, 1984. An Advection-diffusion Concept for Solute Transport in Heterogeneous Unconsolidated Geological Deposits, Water Resources Res., Vol. 21, No. 3, pp. 369-378.

Guven, O., F. J. Molz, and J. G. Melville, 1984. An Analysis of Dispersion in a Stratified Aquifer, Water Resources Res., Vol. 20, No. 10, pp. 1337-1354.

Guven, O., R. W. Falta, F. J. Molz, and J. G. Melville, 1985. Analysis and Interpretation of Single-well Tracer Tests in Stratified Aquifers, Water Resources Res., Vol. 21, No. 5, pp. 676-684.

Intercomp Resource Development and Engineering, Inc., 1976. A Model for Calculating Effects of Liquid Waste Disposal in Deep Saline Aquifers . . . Part I-Development, and Part II-Documentation, prepared for United States Geological Survey (USGS), USGS/WRD/WRI-76-056.

Javandel, I., C. Doughty, and C. F. Tsang, 1984. Ground Water Transport: Handbook of Mathematical Models, American Geophysical Union, Washington, DC.

Lake, L. W., and G. J. Hirasaki, 1981. Taylor's Dispersion in Stratified Porous Media, SPE Journal, Vol. 21, No. 4, pp. 459-468.

Matheron, G., and G. De Marsily, 1980. Is Transport in Porous Media Always Diffusive? A Counterexample, Water Resources Res., Vol. 16, No. 5, pp. 901-917.

Mercado, A., 1984. A Note on Micro and Macro-dispersion, Ground Water, Vol. 22, pp. 790-791.

REFERENCES
(CONTINUED)

Miller, C., T., A. Fischer II, J. E. Clark, W. M. Porter, C. H. Hales, and J. R. Tilton. 1986. Flow and Containment of Injected Wastes, Groundwater Monitoring Review, Vol. 6, No. 3, pp. 37-48, 1986; in Proceedings of International Symposium on Subsurface Injection of Liquid Wastes, March 3 - 5, 1986, New Orleans, Louisiana, pp. 520-559.

Molz, F. J., O. Guven, and J. G. Melville, 1983. An Examination of Scale-dependent Dispersion Coefficients, Ground Water, Vol. 21, No. 6, pp. 715-725.

Muskat, M., 1946. The Flow of Homogeneous Fluids Through Porous Media, J. W. Edwards, Ann Arbor.

Pickens, J. F., and G. E. Grisak, 1981a. Modeling of Scale-dependent Dispersion in Hydrogeologic Systems, Water Resources Res., Vol. 17, No. 6, pp. 1701-1711.

Pickens, J. F., and G. E. Grisak, 1981b. Scale-dependent Dispersion in a Stratified Granular Aquifer, Water Resources Res., Vol. 17, No. 4, pp. 1191-1211.

Taylor, G. I., 1953. Dispersion of Soluble Matter in Solvent Flowing Slowly through a Tube, Prod. Roy. Soc. London, Ser. A, Vol. 219, pp. 186-203.

Taylor, G. I., 1954. Conditions Under Which Dispersion of a Solute in a Stream of Solvent can be used to Measure Molecular Diffusion, Proc. Roy. Soc. London, Ser. A, Vol. 225, pp. 473-477.

FIGURES

Perimeter of Plume from Well No. 2

Fictitious tracer particle for Well No. 2

Perimeter of Plume from Well No. 1

y-velocity component

x-velocity component

Well No. 2

Well No. 1

Fictitious tracer particle for Well No. 1
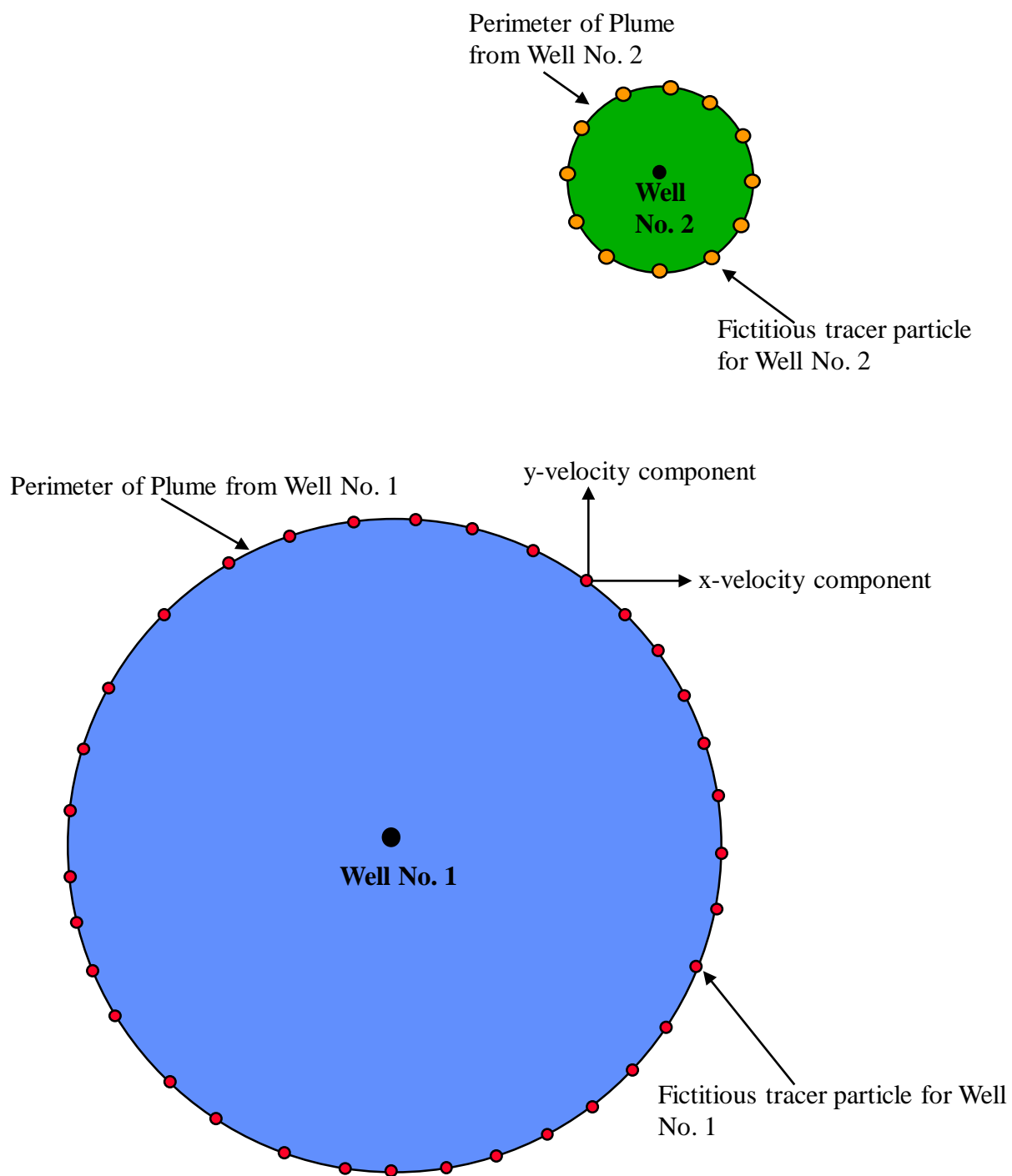
Figure 1
Model Calculation of Fictitious Tracer Particles Around the Perimeters of the Waste Plumes

DuPont

Permeability Variation

Permeability ⟶

Velocity Variation

Lateral Velocity ⟶

Interface between injected and native fluids

Advective Transport

Injected fluid

Native fluid
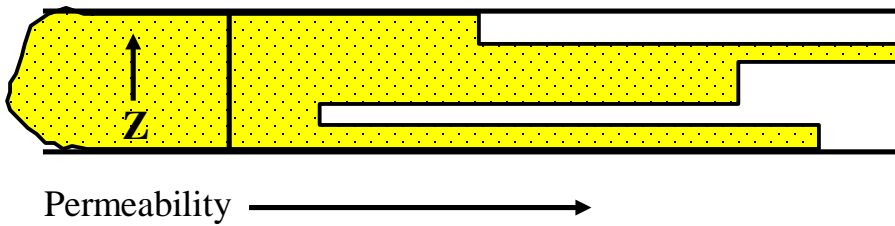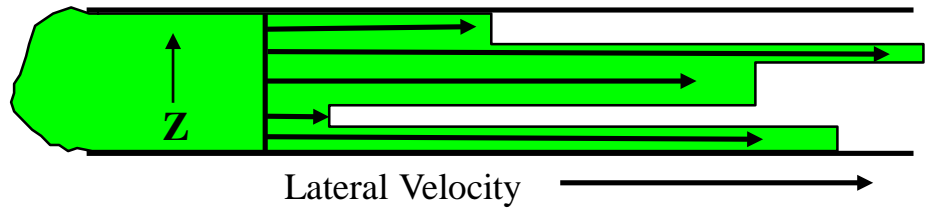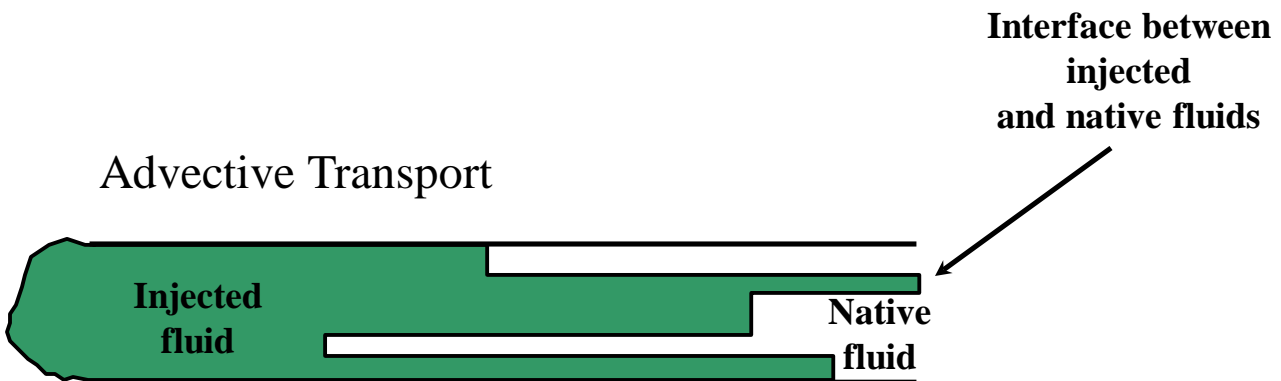
Figure 2
Effect of Stratified Permeability Variations on Lateral Transport
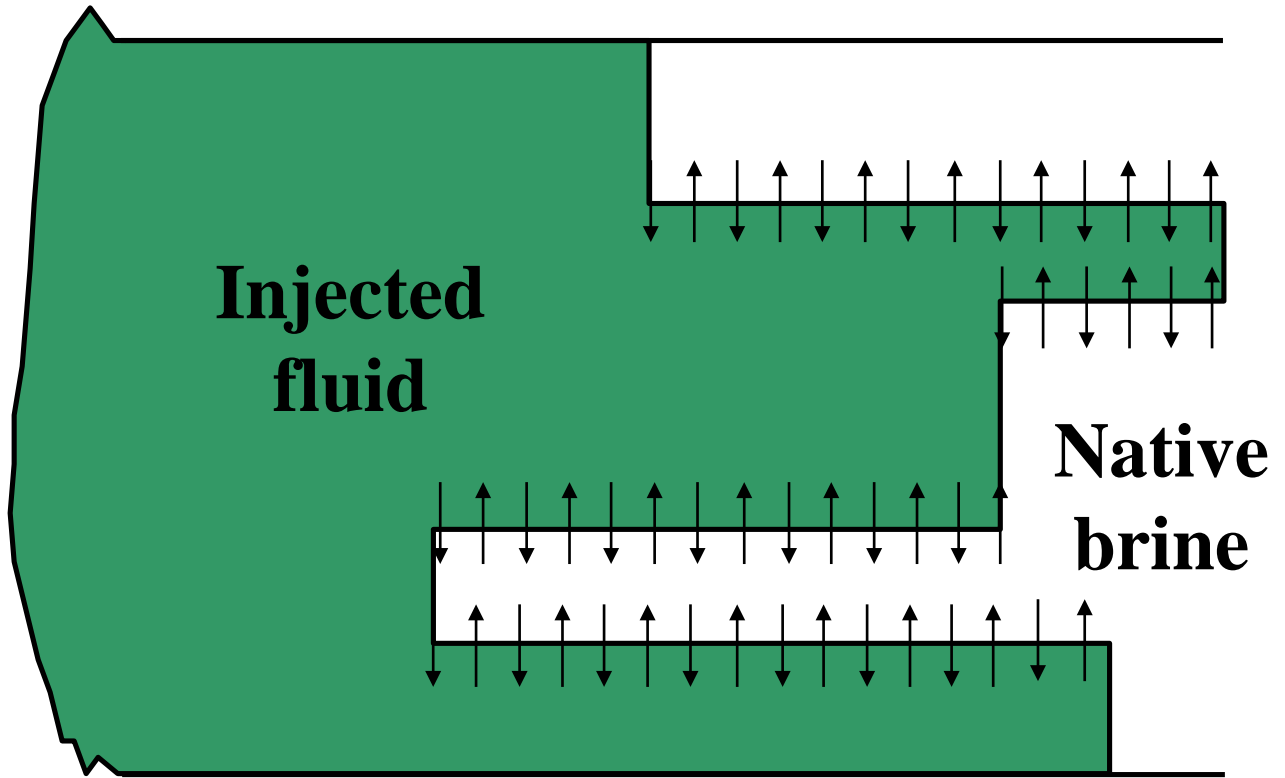
Figure 3
Small-scale Transverse Dispersion Perpendicular to Concentration Fingers
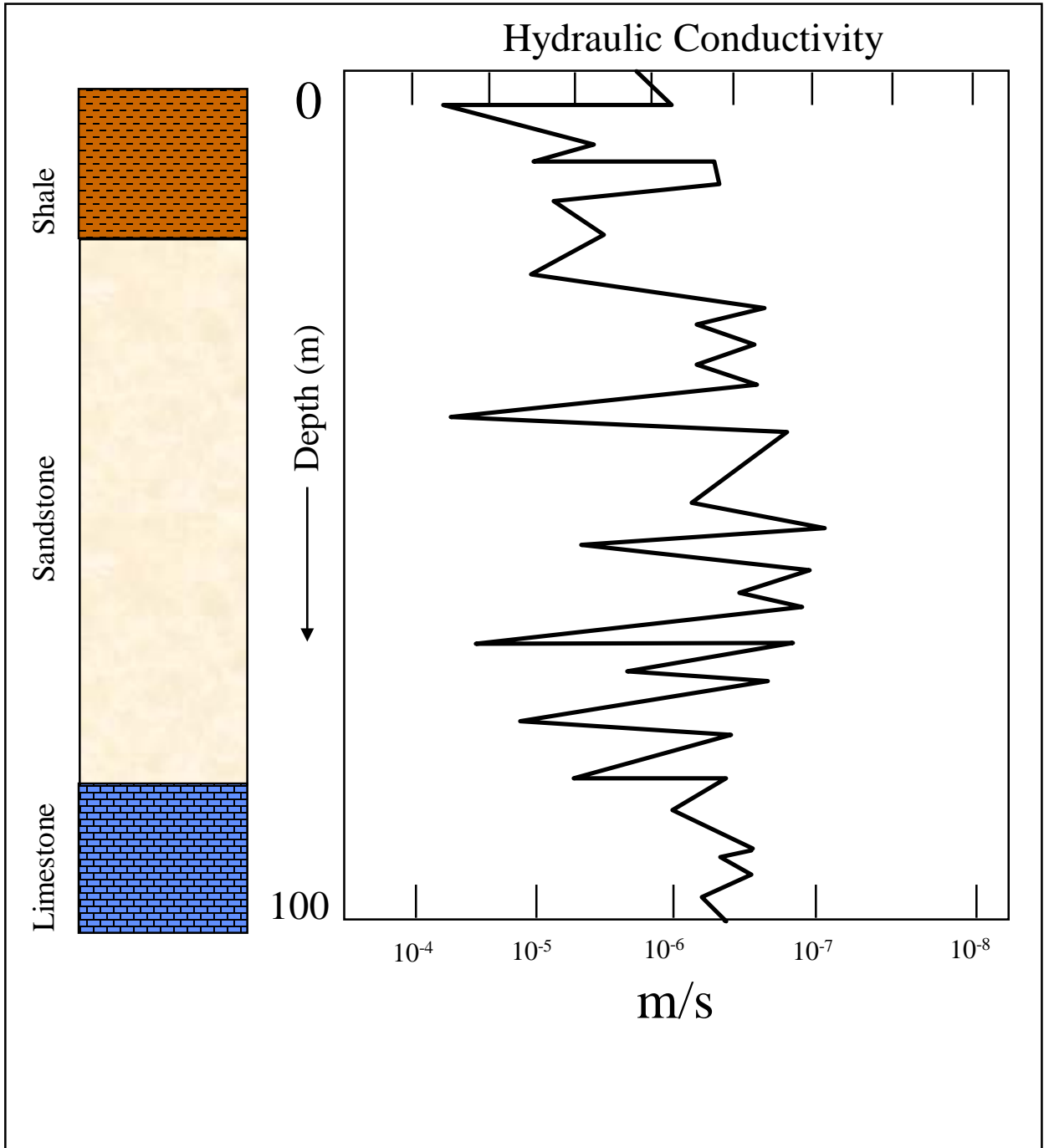
Figure 4
Typical Permeability Variation through the Thickness of a Geological Formation (Freeze and Cherry, 1979). Permeability is Expressed in Terms of Hydraulic Conductivity

$\overline{k}$ = Average horizontal permeability

high pressure
end of slab

low pressure
end of slab

Z

k(z)

permeability profile

$\overline{v}$ = Average horizontal permeability

Z

v(z)
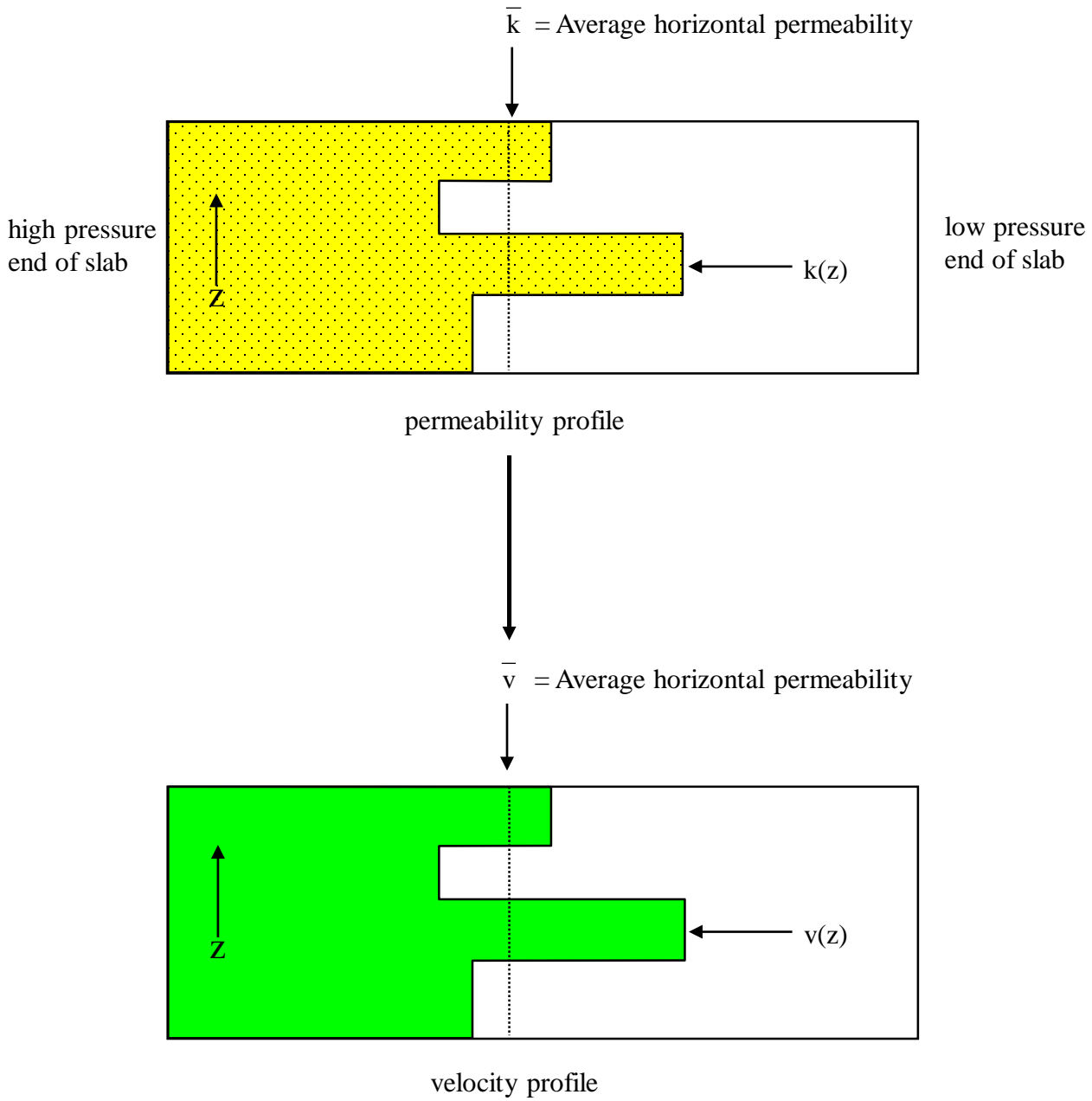
velocity profile

Figure 5
Effect of Stratified Permeability Distribution of Velocity Profile for Rectilinear Flow through a
Porous Slab

← 600 meters →

Well A
(injection)

↕ 600 meters

Well B
(withdrawal)
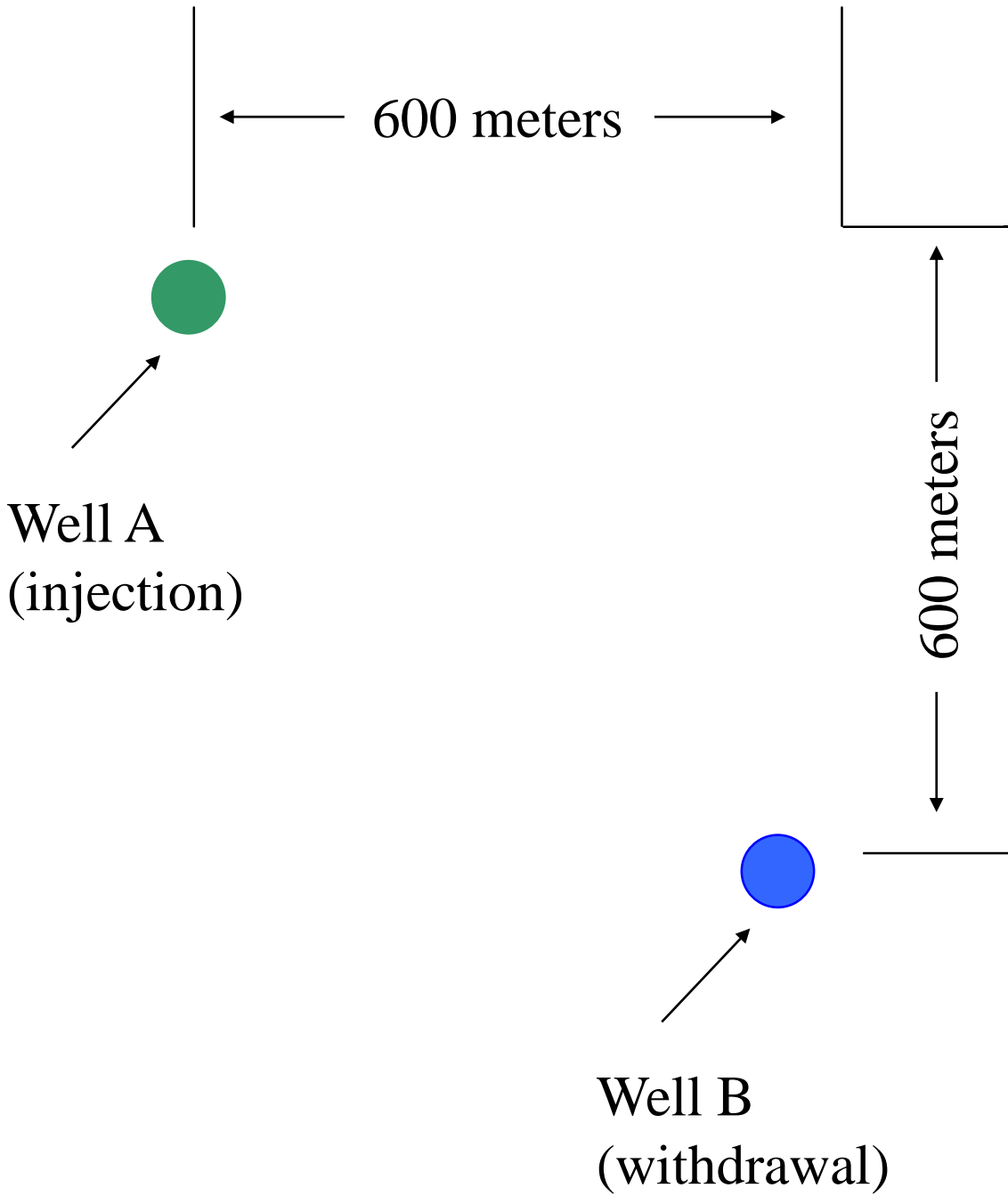
Figure 6
Field Arrangement Analyzed by Javandel et. al., 1984

4 years

2 years

0.5 years

+A

+B

■ Basic Plume Model
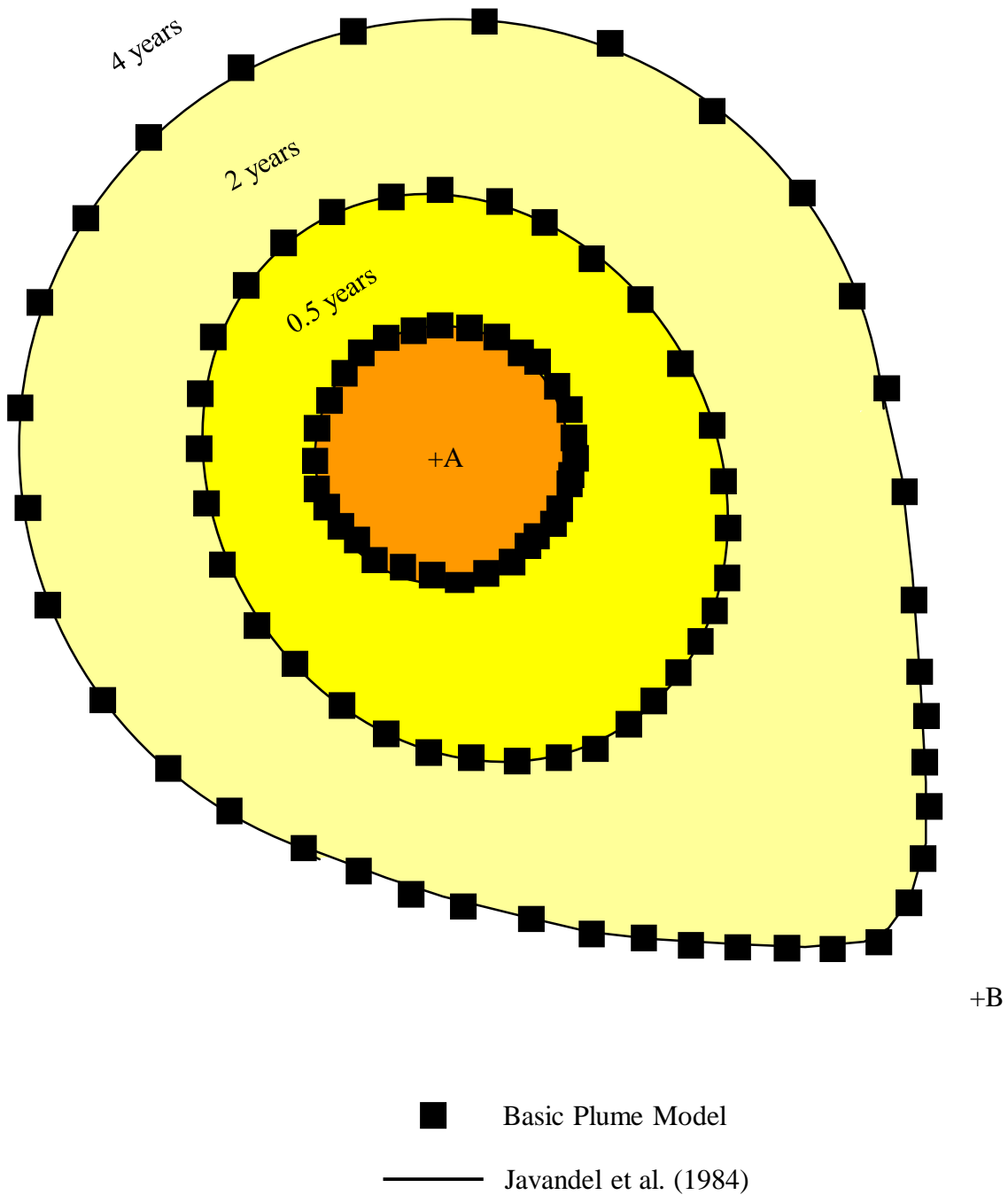
— Javandel et al. (1984)

Figure 7
Comparison of Predicted Plume Shapes at Various Times for the Basic Plume Model and
Results of Javandel et. al., 1984